Plant Physiology Preview. Published on June 1, 2020, as DOI:10.1104/pp.20.00374

Short Title: Cloning of a kernel size QTL in maize

Corresponding author: Jianbing Yan (email: yjianbing@mail.hzau.edu.cn) and David Jackson (jacksond@cshl.edu)
Tel: +86 27 87280110
National Key Laboratory of Crop Genetic Improvement, No.1 Shizishan Street, Hongshan District, Wuhan, Hubei 430070, China.

Title

The kernel size-related quantitative trait locus *qKW9* encodes a pentatricopeptide repeat protein that affects photosynthesis and grain filling

Author names and affiliations

Juan Huang[1], Gang Lu[1], Lei Liu[1,2], Mohammad Sharif Raihan[1], Jieting Xu[1,3], Liumei Jian[1], Lingxiao Zhao[4,5], Thu M. Tran[2,6], Qinghua Zhang[1], Jie Liu[1], Wenqiang Li[1], Cunxu Wei[4], David M. Braun[6], Qing Li[1], Alisdair R. Fernie[7], David Jackson[1,2,*], Jianbing Yan[1,*]

[1]National Key Laboratory of Crop Genetic Improvement, Huazhong Agricultural University, Wuhan 430070, China
[2]Cold Spring Harbor Laboratory, Cold Spring Harbor, NY, USA.
[3]Wimi Biotechnology Co., Ltd, 4th Floor, Kejizhuanhua building, No. 3 Meishan Road, Xinbei District, Changzhou City, Jiangsu Province, China
[4]Jiangsu Key Laboratory of Crop Genetics and Physiology, Co-Innovation Center for Modern Production Technology of Grain Crops, Yangzhou University, Yangzhou 225009, China
[5]Jiangsu Xuzhou Sweetpotato Research Center, Xuzhou, Jiangsu, China
[6]Division of Biological Sciences, Interdisciplinary Plant Group, Missouri Maize Center, University of Missouri, Columbia, MO 65211, USA
[7]Department of Molecular Physiology, Max-Planck-Institute of Molecular Plant Physiology,

Am Mühlenberg 1, 14476 Potsdam-Golm, Germany

One-sentence summary

A pentatricopeptide repeat protein exerts a quantitative effect on maize kernel weight and size by affecting photosynthesis and grain filling.

Funding information

This work was supported by the National Key Research and Development Program of China (2016YFD0100303), the National Natural Science Foundation of China (31525017, 31961133002), and NSF grant IOS-1546837 to DJ; Juan Huang was sponsored by China Scholarship Council to visit Cold Spring Harbor Laboratory and study in Prof. David Jackson's lab from March 2018 to March 2019 (File No. 201706760027).

Author contributions

J.Y. designed and supervised this study. D.J. supervised the study in US side. J.H., G.L., and T. T finished most of the mentioned experiments. Lei. L conducted RNA sequence data analysis. M. S. R. and Jie. L involved in the initial QTL mapping. J.H., G.L. and W. L. performed the field experiments. J.X. and L.J. conducted the transgenic transformation. L.Z. and C.W. performed cytological experiments. Q.Z. constructed the RNA sequencing library and finished the sequencing. J.H., D.B., Q.L., A.F., D.J., and J.Y. contribute a lot of constructive discussions and wrote or revised the manuscript.

Competing financial interests

The authors declare no competing financial interests.

Abstract

In maize (*Zea mays*), kernel weight is an important component of yield, which has been selected during domestication. Many genes associated with kernel weight have been identified

through mutant analysis. Most are involved in the biogenesis and functional maintenance of organelles or other fundamental cellular activities. However, few quantitative trait loci (QTL) underlying quantitative variation in kernel weight have been cloned. Here, we characterize a QTL, *qKW9*, which is associated with maize kernel weight. This QTL encodes a DYW motif pentatricopeptide repeat protein involved in C-to-U editing of *ndhB*, a subunit of the chloroplast NADH dehydrogenase-like complex. In a null *qkw9* background, C-to-U editing of *ndhB* was abolished, and photosynthesis was reduced, which resulted in less maternal photosynthate available for grain filling. Characterization of *qKW9* highlights the importance of optimizing photosynthesis for maize grain yield production.

Keywords

Kernel weight; maize yield; QTL; photosynthesis; Cyclic electron transport; C-to-U editing; NDH complex

INTRODUCTION

Maize (*Zea mays*) is one of the most important crops in the world, producing grain vital for our survival. Along with population growth, environmental deterioration, the decline of arable land and climate change challenge us to increase maize grain production. Therefore, the improvement of maize yield is of great importance to the sustainable development of human society.

The grain yield of maize is comprised of several components, including ear number per plant, kernel number per cob, and kernel weight. As an essential yield component, kernel weight is positively correlated with yield, and is determined during development by kernel size and the degree of kernel filling (Scanlon and Takacs, 2009). To dissect the genetic architecture of maize kernel weight, numerous studies have identified hundreds of quantitative trait loci (QTL) for kernel traits (www.maizegdb.org/qtl). However, only a few kernel size QTL have been cloned and studied, and some maize kernel weight genes have been identified as homologs of rice genes (Li et al., 2010a; Li et al., 2010b; Liu et al., 2015). In one large-scale QTL study in maize, 729 QTL regulating kernel weight-related traits were

85 identified, and 24 of 30 genes were in, or tightly linked to, 18 rice grain size genes, suggesting
86 conserved genetic architecture of kernel weight(Liu et al., 2017b). One example is *teosinte*
87 *glume architecture1* (*tga1*), the causal gene underlying the change from encased kernels in
88 the wild progenitor teosinte to naked kernels in maize(Wang et al., 2005; Wang et al., 2015).
89 Reducing expression of *tga1* in maize by RNAi greatly increases kernel size and weight,
90 suggesting that the removal of glumes from teosinte could release growth constraints, and
91 provide more space to allow larger kernels to develop (Wang et al., 2015). Another kernel
92 size gene, *ZmSWEET4c*, affects kernel weight in a different manner, with its product
93 mediating sugar transport across the basal endosperm transfer cell layer, and shows signals of
94 selection during domestication (Sosso et al., 2015). Recently a further gene, *BARELY ANY*
95 *MERISTEM1d* (*ZmBAM1d*) was identified as an additional QTL responsible for kernel weight
96 variation in maize (Yang et al., 2019).

97 Despite limited progress on our understanding of the quantitative variation in maize
98 kernel weight, numerous kernel mutants have been identified (Neuffer and Sheridan, 1980;
99 Clark and Sheridan, 1991). These mutants have been grouped into three categories: (i)
100 *defective kernel* (*dek*) mutations, including *empty pericarp* (*emp*) mutants that affect both
101 endosperm and embryo; (ii) embryo-specific (*emb*) mutations with healthy endosperm
102 formation; and (iii) endosperm-specific mutations (McCarty, 2017). Mutants in categories i
103 and ii have detrimental effects, leading to substantial loss of kernel weight. Several of these
104 maize kernel development genes have been identified. For instance, *EMP10* (Cai et al., 2017),
105 *EMP11* (Ren et al., 2017), *EMP12* (Sun et al., 2019), *EMP16* (Xiu et al., 2016), *DEK35* (Chen
106 et al., 2017), and *DEK37* (Dai et al., 2018) are involved in intron splicing of mitochondrial
107 genes. In contrast, *MPPR6* functions in maturation and translation initiation of mitochondrial
108 ribosomal protein subunit mRNA(Manavski et al., 2012). Mutations of these genes impair
109 mitochondral function, leading to defective kernels. Other genes, including *EMP7* (Sun et al.,
110 2015), *DEK10* (Qi et al., 2017), *DEK39* (Li et al., 2018), *PPR2263/MITOCHONDRIAL*
111 *EDITING FACTOR29* (Sosso et al., 2012), and *SMALL KERNEL1* (Li et al., 2014) function in
112 C-to-U editing of transcripts in mitochondria and chloroplasts.

113 Many kernel size genes encode pentatricopeptide repeat (PPR) proteins, a large family
114 of RNA-binding proteins in land plants, with more than 400 members in *Arabidopsis*
115 (*Arabidopsis thaliana*), rice (*Oryza sativa*), and maize (*Zea mays*) (Lurin et al., 2004;
116 Schmitz-Linneweber and Small, 2008; Barkan and Small, 2014). Members of the PPR family
117 are characterized by tandem arrays of a degenerate 35-amino-acid motif (PPR motif), and the
118 PPR family is divided into P and PLS subfamilies, according to the nature of the PPR motifs.
119 Members of the P subfamily function in various processes of RNA maturation in organelles,
120 including RNA stabilization, splicing, intergenic RNA cleavage, and translation (Barkan and
121 Small, 2014). The PLS subfamily contains canonical PPR (P) motifs, as well as long (L) and
122 short (S) PPR-like motifs, in a P-L-S pattern. This subfamily is further divided into PLS,
123 E/E+, and DYW classes, based on their C-terminal domains (Barkan and Small, 2014). PLS
124 subfamily members function in RNA editing (Barkan and Small, 2014), a post-transcriptional
125 modification of organelle transcripts, including C-to-U, U-to-C and A-to-I editing
126 (Chateigner-Boutin and Small, 2010; Ruwe et al., 2013; Ruwe et al., 2019).
127 Kernel size and carbohydrate import into kernels directly determine the grain yield of
128 maize, therefore, elucidation of the genetic basis of kernel traits could provide favorable
129 alleles to enhance maize breeding. In a previous study, a maize recombinant inbred line (RIL)
130 population was developed from a cross between two diverse parents, Zheng58 and SK (Small
131 Kernel), which show dramatic variation in kernel weight; and a major kernel weight QTL,
132 *qKW9*, was identified (Raihan et al., 2016; Yang et al., 2019). In this study, we mapped and
133 cloned the causative gene underlying *qKW9,* and identified it as a PLS-DYW type PPR protein
134 coding gene. We found that qKW9 is required for C-to-U editing at position 246 of *ndhB*,
135 encodes a chloroplast-encoded subunit of the NADH dehydrogenase-like (NDH) complex.
136 Functional characterization revealed that C-to-U editing of *ndhB* is crucial for the
137 accumulation of its protein product as well as the activity of the NDH complex. Impairment of
138 this complex led to lower photosynthetic efficiency and a corresponding yield loss of maize in
139 field trials.
140

141 **RESULTS**

142 **Fine mapping and validation of *qKW9***

143 *qKW9* is a major QTL regulating maize kernel weight identified in the ZHENG58×SK RIL
144 population (Raihan et al., 2016). Near-isogenic lines (NILs) harboring the *qKW9* allele from
145 SK or ZHENG58 were screened from RIL-derived heterogeneous inbred families (HIFs) and
146 used to fine map *qKW9*. In contrast to *dek* mutants, which have dramatic kernel weight loss
147 due to defects in the embryo and/or endosperm, the NIL-SK kernels weighed only about 3g
148 less per hundred kernels, compared to NIL-ZHENG58, and their kernel morphology, starch
149 granule structure and plant morphology were similar (Figure 1A-R, Table S1). Thus, the
150 kernel development of NIL-SK plants was not strongly affected. Interestingly, two-week-old
151 seedlings of NIL-SK were smaller than NIL-ZHENG58, possibly as a result of less smaller
152 NIL-SK kernels that provided less nutrition to support their heterotrophic growth that relies
153 on seed derived nutrients (Figure 1B). However, at the mature stage, NIL-SK, and
154 NIL-ZHENG58 plants had similar plant architecture (Figure 1A and 1C). NIL-SK plants had
155 the same kernel row number but fewer kernels per row compared to NIL-ZHENG58 plants ,
156 resulting in smaller ears with fewer kernels (Figure 1D and Table 1).

157 In previous study, line KQ9-HZAU-1341-1 from ZHENG58×SK RIL population with
158 residual heterozygosity was used as founder line to fine map *qKW9.2* (Raihan et al., 2016; Liu
159 et al., 2018). After three generations self-cross and screening against descendents of
160 KQ9-HZAU-1341-1, several recombinant HIFs were obtained. Among the HIFs, F1H5 was
161 used to generate recombination populations to screen for new recombinants to fine map *qKW9*
162 in this study. Eight recombinants was identified by screening 685 F1H5 descendents and they
163 were self-crossed for further analysis (Figure S1). By comparing Hundred Kernel Weight
164 (HKW) of the homozygous progenies from all recombinants, *qKW9* was fine mapped to a ~
165 20kb region defined by markers M3484 and M3506 (156.65Mb and 156.67Mb, respectively in
166 B73 RefGen v4) (Figure 2A and Fig S1). Three genes (*Zm00001d04850*, *Zm00001d048451*,
167 and *Zm00001d048452*) were annotated within this region in B73 RefGen v4 (Figure 2B).
168 Several SNPs were found in *Zm00001d04850*, however they were all synonymous. The second

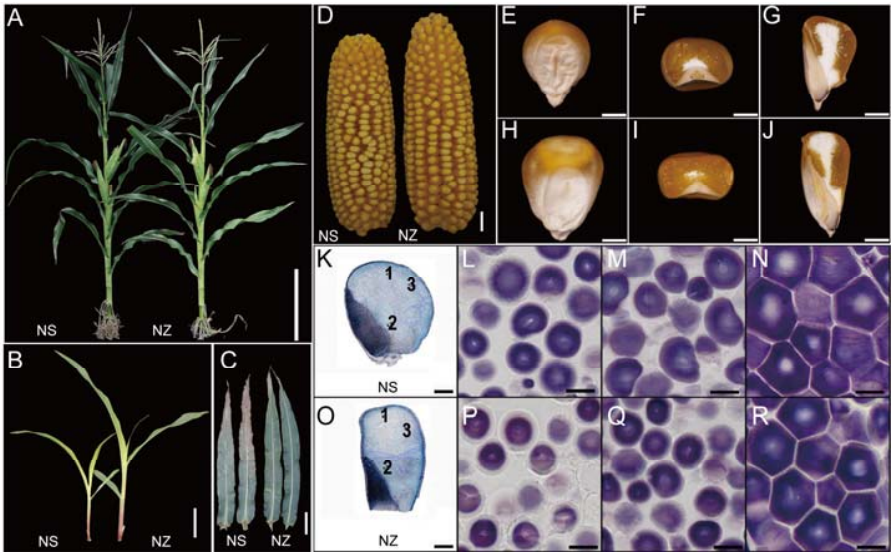

gene, *Zm00001d048451*, had a 13bp deletion in coding sequence of SK, possibly leading to loss of function (Figure 2C). We failed to amplify the third gene, *Zm00001d048452*, from both SK and ZHENG58, and therefore, screened SK and ZHENG58 BAC libraries to search for sequence variation. However, sequence alignment and annotation revealed that *Zm00001d048452* was absent from both SK and ZHENG58, and there were no additional annotated genes within the *qKW9* locus, although there were some large-fragment insertions or deletions in the intergenic regions (Figure 2B). These results were further verified using the assembled SK genome (Yang et al., 2019). Of the two remaining candidates, *Zm00001d048450* displayed neither change in expression level nor pattern (Figure S2A), which together with its lack of non-synonymous SNPs suggested *Zm00001d048451* to be the causative gene of *qKW9*.

To validate *Zm00001d048451* as the gene underlying *qKW9*, we adopted the CRISPR/Cas9 system to create knockout mutants (Figure 2C). Editing of *qKW9* was identified by Sanger sequencing of T_0 transgenic plants, and two null mutants, *qkw9-cr1*, carrying a 1bp-deletion, and *qkw9-cr2*, carrying a 4bp-deletion, were used for subsequent analysis (Figure 2C and Figure 3). For both alleles, we found that kernel weight and ear weight were reduced compared to their corresponding wild type (Figure 3), demonstrating that *Zm00001d048451* was indeed the causative gene of *qKW9*.

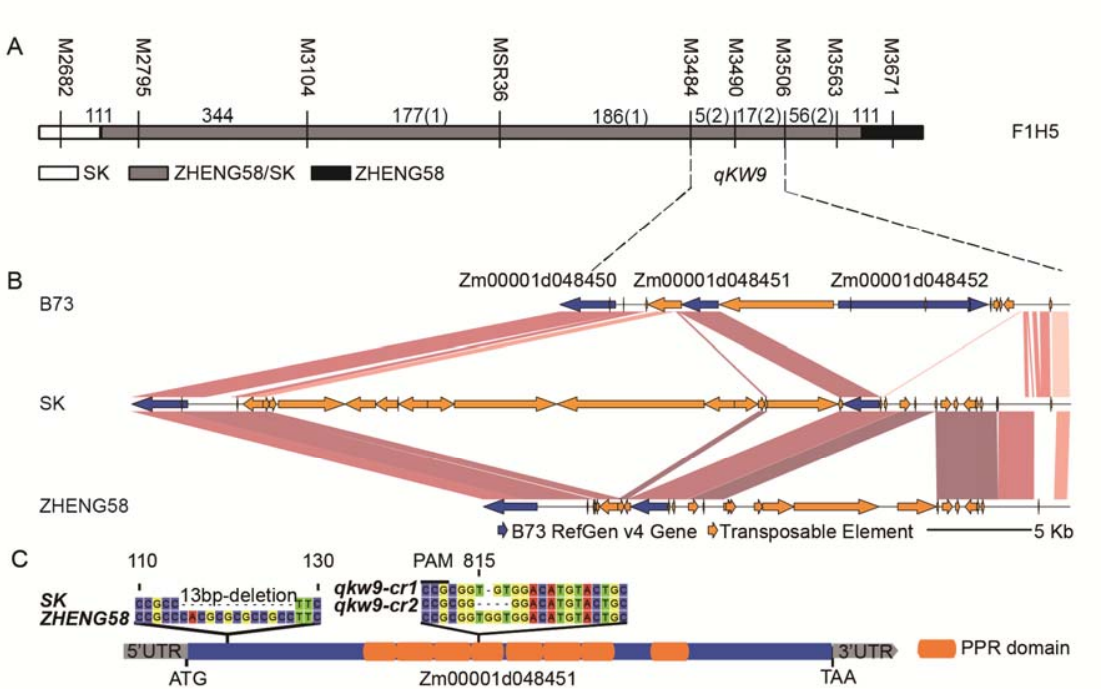

Maize kernel weight is determined by endosperm development and grain filling after fertilization, and can be heavily influenced by maternal influences, such as supply of photosynthate from source tissues. To address if *qKW9* controls kernel weight by a maternal effect, we measured kernel weight from selfed ears of NIL-ZHENG58 or NIL-SK, as well as from reciprocal F1 ears NIL-ZHENG58×NIL-SK, or NIL-SK×NIL-ZHENG58. We also measured *qkw9-cr1*/+ selfed and *qkw9-cr2*/+ selfed (Figure S3A). The kernel weight was not significantly different between NIL-ZHENG58 selfed and NIL-ZHENG58×NIL-SK, as well as between between NIL-SK selfed and NIL-SK×NIL-ZHENG58 (Figure S3B). The kernels also showed uniform size on the ears of F1 (NIL-ZHENG58×NIL-SK), *qkw9-cr1*/+ and *qkw9-cr2*/+ selfed (Figure S3A). These results suggest that *qKW9* controls kernel weight majorly by the maternal effect, and the *qKW9* may play function in the maternal tissues.

qKW9 is highly expressed in leaf, and encodes a chloroplast protein involved in _ndhB_ RNA editing

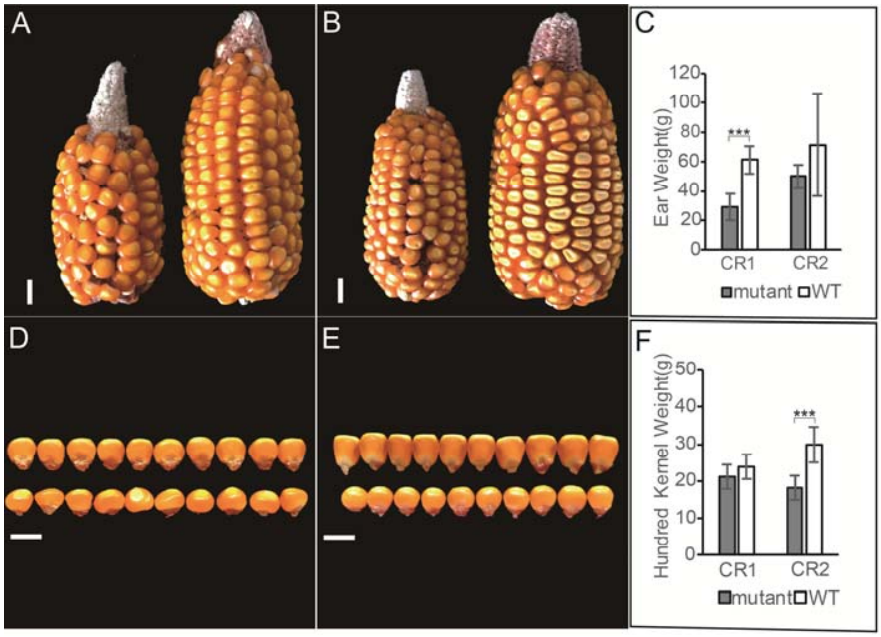

Zm00001d048451/*qKW9* is predicted to encode a DYW subgroup pentatricopeptide repeat (PPR) protein with eight putative PPR motifs (Figure 2C). An Arabidopsis ortholog, *AT5G66520* (Figure 4A) encodes a DYW subgroup protein with ten PPR motifs and was designated *Chloroplast RNA Editing Factor 7* (*CREF7*), functioning in *Ndh* editing (Yagi et al., 2013). In order to address if *qKW9* is also involved in chloroplast RNA editing, we analyzed its expression and subcellular localization. Real-time PCR of *qKW9* revealed a considerably higher expression level in leaf than in other tissues (Figure S2B). *qKW9* expression was detected in all leaf-related tissues, and its expression level (13.9-87.6 FPKM) was much higher than in other tissues (0-12.8 FPKM) (Stelpflug et al., 2016). To test the subcellular localization of *qKW9*, we transiently expressed a *qKW9*-GFP fusion protein in tobacco (*N. tabacum*), and found localization in the stroma of chloroplasts (Figure 4B–E), agreeing with a chloroplast prediction by TargetP (Emanuelsson et al., 2007).

To evaluate RNA editing by *qKW9*, leaves from NIL-SK and NIL-ZHENG58 plants before and after pollination were collected for total RNA sequencing. By comparing editing frequencies between NIL-SK and NIL-ZHENG58, six loci putatively edited by *qKW9* were identified with p-value < 0.05 and mean editing frequency difference > 5% (Table 2). Three of these loci at chloroplast genome positions 90736, 132001, and 65407 (B73 RefGen v4), had

217 striking editing differences between NIL-SK and NIL-ZHENG58, with close to 100% editing
218 in NIL-ZHENG58 but almost none in NIL-SK at all stages tested (Table 2). Position 65407 is
219 in an intergenic region, whereas positions 90736 and 132001 are in the 246th codon of

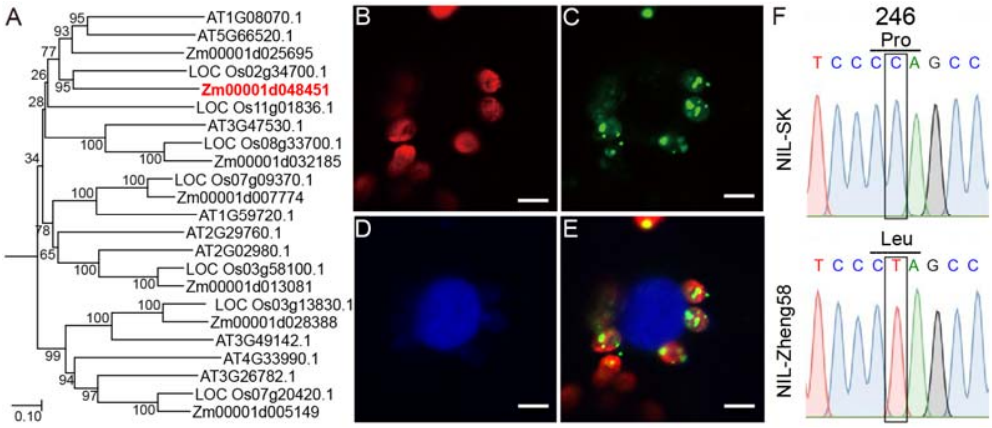

220 *GRMZM5G876106* and *GRMZM5G810298,* respectively (Table 2). These genes are the two
221 copies of *ndhB* in the chloroplast genome, and their C-to-U editing changes the 246th amino
222 acid from proline to leucine. Thus, the sites edited by qKW9 were designated as *NdhB-246*.
223 We confirmed the *NdhB-246* editing difference by Sanger sequencing in NIL-SK and
224 NIL-ZHENG58 (Figure 4F). We also investigated the editing frequency of *ndhB-246* in
225 leaves of our two CRISPR/Cas9 null mutants, as expected, *ndhB-246* editing being abolished
226 in both mutants. These results demonstrate that *qKW9* is essential for *ndhB-246* editing.

227 RNA editing defects may directly alter protein function or affect its ability to form
228 complexes with other proteins (Hammani et al., 2009). *ndhB* encodes a subunit of the NDH
229 complex (Laughlin et al., 2019), so we asked if this complex accumulates in the null *qkw9*
230 background using protein blots probed with antibodies against NdhH to monitor
231 accumulation of the complex. In NIL-SK, the level of NdhH was reduced to less than 25% of
232 NIL-ZHENG58 (Figure 5), suggesting that *ndhB-246* RNA editing by *qKW9* is important for
233 normal accumulation of the NDH complex.

234 **C-to-U editing of *ndhB-246* is essential for optimal activity of NDH complex, electron**
235 **transport rate and non-photochemical quenching induction**

236 The chloroplast NADH dehydrogenase-like (NDH) complex transfers electrons

237 originating from Photosystem I (PSI) to the plastoquinone pool, while concomitantly
238 pumping protons across the thylakoid membrane (Strand et al., 2017). Its activity can be
239 monitored as a transient increase in chlorophyll fluorescence, reflecting plastoquinone

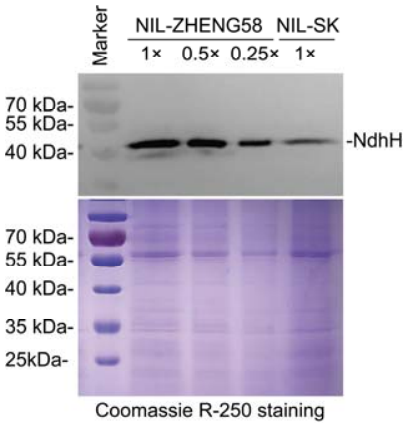

240 reduction after turning off actinic light (AL) (Burrows et al., 1998; Shikanai et al., 1998). In
241 Arabidopsis, several nuclear mutants affecting NDH activity function in RNA processing of
242 NDH subunit transcripts. For instance, *Chlororespiratory Reduction 2* (*CRR2*) functions in
243 the intergenic processing of chloroplast RNA between *rps7* and *ndhB* (Hashimoto et al.,
244 2003). A null allele of *CRR2* lacks NDH activity, and the post-illumination increase in
245 chlorophyll fluorescence is undetectable, with a similar phenotype being observed in the
246 tobacco (*N. tabacum*) *ndhB* mutant (Hashimoto et al., 2003).

247 To check whether *qKW9* impaired NDH activity, we monitored chlorophyll fluorescence
248 using the post-illumination method (Burrows et al., 1998; Shikanai et al., 1998). The
249 measurement was conducted using the mature leaf beside the ear at the 30 days after
250 pollination (DAP) in the normal field. Figure 6A shows a chlorophyll fluorescence trace from
251 wild-type maize and *qkw9-cr1* and *qkw9-cr2*. In both *qkw9-cr1* and *qkw9-cr2*, the
252 post-illumination increase of chlorophyll fluorescence was reduced, indicating that NDH
253 activity was diminished in the null *qkw9* background, and that the Leu residue at position 246
254 of ndhB protein is required for NDH accumulation and activity. We next measured
255 non-photochemical quenching (NPQ), a chlorophyll fluorescence parameter indicative of the
256 level of thermal dissipation. NPQ was induced with increasing light intensity in both *qkw9*-cr1

257 and wild type prior to saturation of the ETR (Figure 6B). However, its induction in *qkw9*-cr1
258 was significantly lower at light intensities of 2413 μmol m^{-2} s^{-1}, indicating that thermal
259 dissipation was impaired in *qkw9*-cr1(Figure 6B). ETR represents the relative flow of

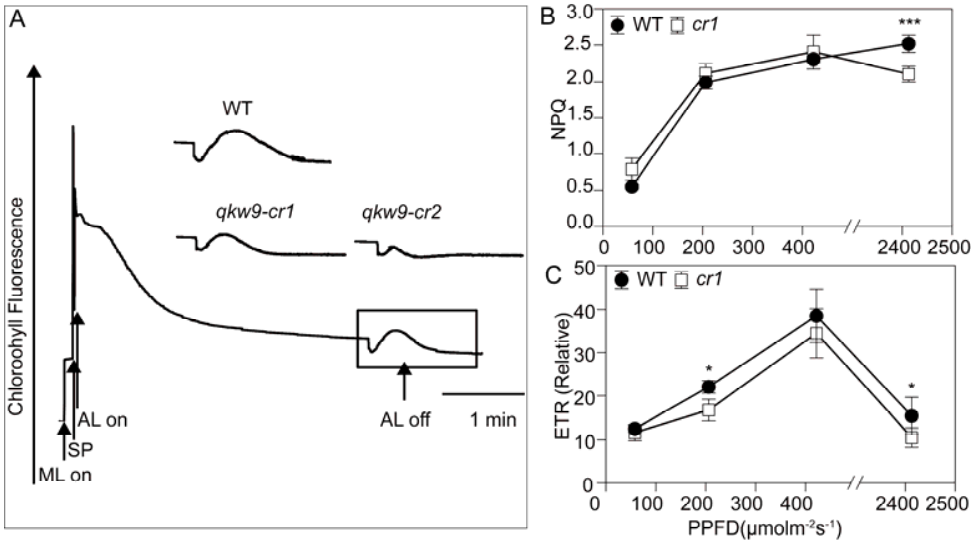

260 electrons through PSII during steady-state photosynthesis. It increases with increases in light
261 intensity until a point at which it cannot be further increased – termed its saturation point. For
262 both wild-type and *qkw9*-cr1, the saturation point was over 400 μmol m^{-2} s^{-1} (Figure 6C).
263 Whilst, ETR was not affected in *qkw9-cr1* at a low light intensities of ~100 μmol m^{-2} s^{-1}
264 (Figure 6C), it tended to be lower in *qkw9-cr1* at intensities above this (significantly so at 200
265 and 2400 μmol m^{-2} s^{-1}). The ETR was also observed reducing when the light intensities
266 increased from 400 to 2400 μmol m^{-2} s^{-1}, which probably caused by the photodamage under
267 high intensity of light. As the leaf senescence was greater in *qkw9* than WT at 30 DAP, it was
268 possible that the reduction in NPQ and ETR might be caused by more severe photodamage in
269 the *qkw9* null allele. These results also implied that the NDH-dependent photoprotection
270 involved in photosynthesis maintenance to produce glucose for grain filling (Peterson et al.,
271 2016), which is consistent with the overall reduced grain yield in NIL-SK considering that
272 light intensity is far in excess of 100 μmol m^{-2} s^{-1} in the field.

273 ***qkw9* reduces kernel weight by affecting photosynthesis**

274 Genetic evidence suggests that physiological functions of cyclic electron transport (CET)

275 around Photosystem I (PSI) are essential for efficient photosynthesis and plant growth
276 (Munekage et al., 2004). The physiological role of CET is to protect PSII under intense light
277 via ΔpH-dependent thermal dissipation in PSII, as well as to act as an ATP generator in
278 photosynthesis (DalCorso et al., 2008; Alric and Johnson, 2017). Our results suggest that
279 reduced activity of the NDH complex in maize affected NPQ and ETR. We therefore asked
280 how photosynthesis and carbon assimilation were affected by changes in NDH activity? We
281 measured the fresh weight of developing kernels of NIL-SK and NIL-ZHENG58 under field
282 conditions, and investigated several photosynthesis-related parameters (Figure 7). Fresh
283 weight of NIL-SK kernels was similar to NIL-ZHENG58 before 30 DAP (Figure 7A).
284 However, kernels of NIL-SK reached their maximum fresh weight at 30 DAP, while
285 NIL-ZHENG58 kernels continued to gain weight until 35 DAP, suggesting that carbon
286 deposition in kernels was greater in NIL-ZHENG58 at 35 DAP (Figure 7A). Consistent with
287 this observation, leaves of NIL-SK had more severe senescence at 30 DAP compared to
288 NIL-ZHENG58, indicating decreased source strength in the NIL-SK plants (Figure 1C).
289 NIL-SK also had significantly lower net photosynthesis than NIL-ZHENG58 at 22 DAP and
290 30 DAP (Figure 7B). Consistently, stomatal conductance and transpiration rate were similarly
291 lower in NIL-SK than in NIL-ZHENG58 (Figure 7C-7D). The lower photosynthetic capacity
292 of NIL-SK, coupled with the potential compensatory fact that less kernels were produced per

293 ear in this line (Table 1), may explain why the fresh weight of NIL-SK were not significantly
294 lower than NIL-ZHENG58 at 22 DAP and 30 DAP (Figure 7A). In addition, the chlorophyll
295 content (SPAD value) and the maximum efficiency of PSII (Fv/Fm) were invariant between
296 the NILs (Figure 7E-7F), indicating that the differences in the net photosynthetic rates might
297 not result from a different level of photosynthesis potential. Accordingly, the photosynthetic
298 rate was also significantly lower in *qKW9*-cr1 than WT at 30 DAP under field conditions
299 (*qKW9*-cr1: 17.35±2.10 μmol $CO_2 m^{-2}s^{-1}$, Wild type: 29.68±3.56μmol CO_2 $m^{-2}s^{-1}$, *n*=6). We
300 conclude that impaired NDH activity affected both net photosynthesis and the duration of
301 active photosynthesis, resulting in smaller ears and kernels in NIL-SK. Although the lost of
302 RNA editing of *ndhB* impacts photosynthesis in *qkw9* null allele, it doesn't affect the normal
303 growth of plant, and the shorter duration of active photosynthesis may contract the growth
304 cycle for rapid reproduction. So the null *qkw9* can be kept in the small kernel inbred line SK
305 (Yang et al., 2019).
306

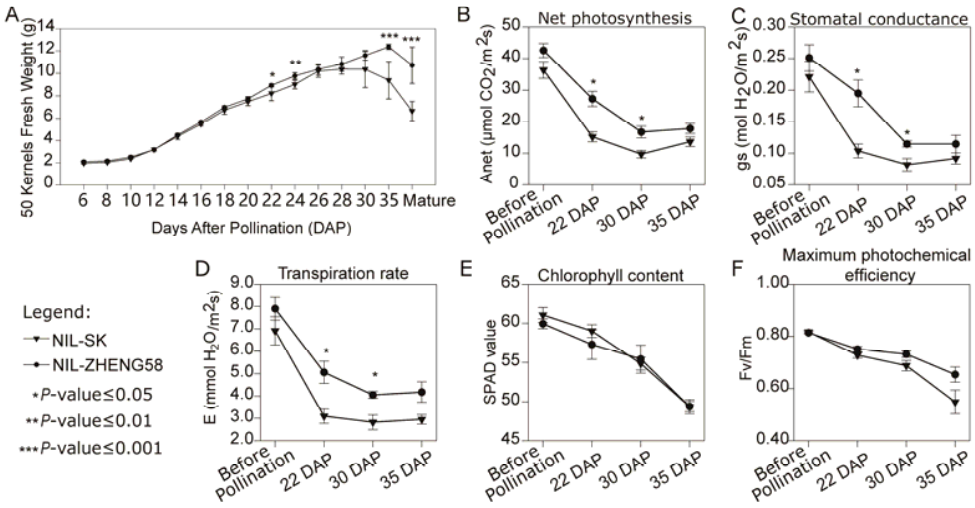

307 **DISCUSSION**

308 ***qKW9* encodes a PPR gene responsible for C-to-U editing of *ndhB***

309 The maize kernel has been of interest to researchers as a model system for the study of
310 development and genetics for a century. Numerous kernel mutants have been identified
311 (Neuffer and Sheridan, 1980; Sheridan and Neuffer, 1980; Clark and Sheridan, 1991), and in
312 recent years, many mutants that result in dramatically reduced kernel size, and seedling
313 lethality have been identified. In many cases, *PPR* genes are responsible for these phenotypes,
314 due to their function in organellar gene expression. Generally, null alleles of PPR genes in
315 previous studies produce kernels that are with obvious development abnormality at early stages
316 and are easily distinguished from normal kernels on self-crossed F_1 ears due to their smaller
317 size, pale pericarp, flat or shrunken appearance (Manavski et al., 2012; Sosso et al., 2012; Li et
318 al., 2014; Sun et al., 2015; Xiu et al., 2016; Cai et al., 2017; Chen et al., 2017; Qi et al., 2017;
319 Ren et al., 2017; Dai et al., 2018; Li et al., 2018; Sun et al., 2019). Unlike these kernel mutants,
320 kernels produced by null allele of *qKW9* are similar in appearance and viability although
321 smaller in size comparing to wild type, and kernel weight is determined by genotype of
322 maternal plant rather than kernel genotype. *qKW9* is the C-to-U editing factor in the maize
323 chloroplast that has a quantitative rather than qualitative effect on kernel and ear size. This
324 difference stems from the involvement of *qKW9* in the abundance of the NDH complex, which
325 in known to play a regulatory role in photosynthesis (Nashilevitz et al., 2010; Peltier et al.,
326 2016; Peterson et al., 2016). Based on results from this study, it is possible that variants of
327 other yet-unidentified RNA editing factors responsible for the 11 C-to-U editing sites in maize
328 *ndh* transcripts will also affect kernel and ear size in a quantitative way. Indeed, studies in
329 *Arabidopsis* have identified many PPR genes affecting *ndh* expression, by focusing on
330 changes in chlorophyll fluorescence related to NDH activity (Kotera et al., 2005; Okuda et al.,
331 2007; Hammani et al., 2009; Okuda et al., 2010).

332 Plastid genomes encode 11 subunits (NdhA to NdhK) forming the core of the membrane
333 arm of the L-shaped structure of the NDH complex (Laughlin et al., 2019). In Arabidopsis,
334 the PPR proteins, those regulate the *ndh* genes expression, are either responsible for splicing

335 of polycistronic transcripts, or site-specific C-to-U RNA editing (Hashimoto et al., 2003;
336 Munekage et al., 2004; Kotera et al., 2005; Okuda et al., 2007; Hammani et al., 2009; Okuda
337 et al., 2009; Okuda et al., 2010). C-to-U RNA editing is important in organelle gene
338 expression in various organisms, although the efficiency varies in different organs and at
339 different developmental stages (Maier et al., 1995; Peeters and Hanson, 2002). C-to-U RNA
340 editing in Arabidopsis can generate translational initiation codons, as in *CRR4* (Kotera et al.,
341 2005) or cause amino acid alterations, as in *CRR21*, *CRR22*, *CRR28*, *OTP82*, *OTP84* and
342 *OTP85* (Okuda et al., 2007; Hammani et al., 2009; Okuda et al., 2009; Okuda et al., 2010).
343 Editing of *ndhB-246* in leaf tissues is near 100% in maize, suggesting that it is important for the
344 function of ndhB protein (Peeters and Hanson, 2002). *ndhB-246* editing also occurs in tobacco
345 and rice (Tsudzuki et al., 2001). Therefore, C-to-U editing of *ndhB-246* appears crucial to its
346 function. The *qKW9* QTL characterized in our study is the RNA editing factor that has been
347 linked to C-to-U editing of *ndhB-246*. Our results clearly indicate that the abolition of C-to-U
348 editing in *ndhB-246* impairs accumulation of the NDH complex *in vivo*.

349 **NDH complex may play more important role in C_4 than C_3**

350 In the light reactions of photosynthesis, linear electron transport (LET) from water to
351 $NADP^+$ does not fully satisfy the ATP/NADPH production ratio required by the
352 Calvin-Benson cycle and photorespiration (Yin and Struik, 2018). Cyclic electron transport
353 (CET) around photosystem I (PSI) has, therefore, been considered as a candidate for
354 augmented ATP synthesis in response to fluctuating demand during photosynthesis (Rumeau
355 et al., 2007; DalCorso et al., 2008; Nakamura et al., 2013). In PSI CET, electrons are recycled
356 around PSI generating ΔpH and consequently ATP without a concomitant accumulation of
357 NADPH (Shikanai, 2007; Munekage and Taniguchi, 2016). In Arabidopsis, two CET
358 pathways have been identified by genetics, and the main pathway depends on PROTON
359 GRADIENT REGULATION 5 (PGR5)/PGR5-LIKE PHOTOSYNTHETIC PHENOTYPE 1
360 (PGRL1) proteins, whereas the minor pathway is mediated by the chloroplast NADH
361 dehydrogenase-like (NDH) complex (Munekage et al., 2002; Munekage et al., 2004;
362 DalCorso et al., 2008). Chloroplast NDH mediation of CET around PSI was first reported in

363 tobacco following disruption of *ndhB* (Shikanai et al., 1998; Burrows et al., 1998). Knockout
364 lines of *ndh* genes were created by plastid transformation in tobacco. Mutants defective in
365 expression of chloroplast *ndh* genes were isolated in Arabidopsis (Hashimoto et al., 2003).
366 However, both knockout lines of *ndh* genes in tobacco and mutants with impaired NDH
367 activity in Arabidopsis lack morphological phenotypes (Hashimoto et al., 2003; Munekage et
368 al., 2004; Okuda et al., 2007; Hammani et al., 2009; Okuda et al., 2009; Okuda et al., 2010).
369 So, the general conclusion has been that mutants defective in NDH do not show a clear
370 phenotype and NDH is dispensable at least when plants are grown in controlled environments
371 in C_3 system. In the C_4 system, the maize *Ndh* mutant showed slower growth and
372 photosynthesis, reduced pigment levels, and substantial effects on indicators of PSII function,
373 compared to normal lines (Peterson et al., 2016). In the *qkw9* null alleles, the impaired NDH
374 activity also resulted in smaller ears and kernels. The phenotype of maize *Ndh* mutant was
375 sugeested to be a secondary consequence of the much lower Bundle Sheath Cell CO_2
376 concentrations attainable, and the lower Bundle Sheath Cell CO_2 concentrations was also
377 observed in *qkw9* null alleles (Figure 7B). CET around photosystem I is critical for balancing
378 the photosynthetic energy budget of the chloroplast by generating ATP without net production
379 of NADPH (Ishikawa et al., 2016a). C_4 plants have higher ATP requirements than C_3 plants
380 (Ishikawa et al., 2016b), rendering the ATP supply by CET particularly important, imply that
381 during the evolution of NADP-malic enzyme-type C_4 photosynthesis in the C_4-like genus
382 *Flaveria*, CET was promoted by markedly increasing expression of both PGR5/PGRL1 and
383 NDH subunits (Nakamura et al., 2013). The NDH subunit, however, increases markedly in
384 bundle sheath cells with the activity of the C_4 cycle while PGR5/PGRL1 increases in both
385 mesophyll and bundle sheath cells in *Flaveria* and other C_4 species, implying that the NDH
386 complex provides a considerable role in the establishment of C_4 photosynthesis (Nakamura et
387 al., 2013). Previously, it was also shown that NDH plays a central role in driving the
388 CO_2-concentrating mechanism in C_4 photosynthesis (Takabayashi et al., 2005; Andrews,
389 2010; Peterson et al., 2016). In addition, the NDH complex has been experimentally
390 demonstrated to be a high-efficiency proton pump, increasing ATP production by cyclic

391 electron transport (Strand et al., 2017). Ishikawa et al. report that NDH-suppressed C_4 plants
392 are characterized by consistently decreased CO_2 assimilation rates, impaired proton
393 translocation across the thylakoid membrane and reduced growth rates (Ishikawa et al.,
394 2016a), which was also been observed in the maize *Ndh* mutants (Peterson et al., 2016).
395 Therefore, our study of *qKW9* also provides a possible explanation for the apparent
396 contradiction of these observations, in suggesting that the NDH complex is more important in
397 C_4 than in C_3 plants on photosynthetic efficiency, which is consistent with previous study by
398 using maize *Ndh* mutants (Peterson et al., 2016).

399 **The photosynthetic efficiency is crittical for the grain productivity of crops**

400 Grains are typical sink organs -i.e. they are net receivers of photoassimilates from
401 photosynthetically active source tissues - and a considerable number of studies suggest that
402 enhancing photosynthetic efficiency could increase the productivity of crops (Sonnewald and
403 Fernie, 2018; South et al., 2019; Wu et al., 2019). In the *qkw9* null allele, the overall rate of
404 photosynthesis was reduced, which might be caused by lower accumulation of the NDH
405 complex (Figure 5) as its critical function on CO_2 concentration (Peterson et al., 2016), that
406 lead to significantly reduced ear and kernel size. As in maize *Ndh* mutants, the NPQ was also
407 significantly affected in *qkw9* null allele NIL-SK, but the influence was minor, the possible
408 reason is that the chlorophyll fluorescence is mainly from mesophyll cells and indirectly
409 impacted by mild reduction in CO_2 fixation in bundle sheath cells (Figure 7B) (Peterson et al.,
410 2016). However, the *qkw9* null allele plants displayed higher levels of leaf senescence in the
411 late stage of grain filling, a phenomenon that may result from the photoprotective quenching
412 by the NDH-dependent H+-translocating cyclic pathway in the mesophyll cell chloroplasts
413 (Peterson et al., 2016). This matched the stage when NIL-SK plants had lower fresh kernel
414 weight than NIL-ZHENG58 plants (Fig 7A). This result suggests that NDH-dependent
415 photoprotection is also critical for the maintenance of photosynthesis and therefore continued
416 production of glucose for grain filling. As such the enhancement of NDH-dependent
417 photoprotection may extend the time window of photosynthesis and grain filling after
418 pollination, and thereby lead to a higher grain yield production. This study thus further

419 confirms current models of the role of the NDH in C4 photosynthesis, and suggests a novel
420 potential strategy for crop improvement.

421 **MATERIALS AND METHODS**

422 **Fine mapping of *qKW9***

423 Multiple major QTL regulating kernel-size-related traits were identified by
424 multi-environment QTL analysis in ZHENG58×SK RIL population and a major QTL on
425 chromosome 9 regulating kernel width was designated as *qKW9* in a previous report (Raihan et
426 al., 2016). The Zheng58 is an elite inbred line used widely in commercial maize breeding
427 program in china, in contrast, the SK inbred line selected from tropical landraces with a very
428 small kernel size (Raihan et al., 2016) and its genome was well assembled recently (Yang et
429 al., 2019). To fine-map *qKW9*, the heterogeneous inbred family (HIF) was screened against the
430 RIL population and RIL line KQ9-HZAU-1341-1 was heterozygous between Marker M2682
431 (155.83Mb in B73 Ref Gen v4) and Marker M3671 (156.83Mb in B73 RefGen v4) was used
432 as the founder HIF (Raihan et al., 2016). In a nursery grown in Hainan in 2015, two groups of
433 homozygous progenies of F1H5, which was a descendant of line KQ9-HZAU-1341-1, were
434 significantly different in hundred kernel weight (HKW), kernel length (KL), and kernel width
435 (KW). Thus, F1H5 was used as the starting HIF to fine map *qKW9* in this study. In the summer
436 of 2016, recombinants between Marker M2795 and Marker M3671 were screened against the
437 F1H5 population. In the winter of 2016, progeny tests were conducted on those recombinant
438 populations.

439 For genotyping, genomic DNA extraction from young leaf was conducted using the CTAB
440 protocol for plant tissues. To detect SNP and Indel markers, PCR was conducted in 10 μL
441 reactions with KASP master mix (cat no: KBS-1030-002, LGC), self-made KASP array mix,
442 and DNA template in 96 well non-transparent plates. KASP array mix was made by mixing
443 equal volumes of primer F1 (36 μM), F2 (36 μM), and R (90 μM) of a specific SNP marker. For
444 each reaction, 0.14 μL array mix, 1×master mix, and 20~200 ng DNA were used. Thermal
445 cycling was 94°C for 15 minutes to activate the enzyme, followed by 10 cycles of touch down
446 PCR (denature at 94°C for 20 s, annealing/elongation start with 61°C for 60 s, drop 0.6°C per

447 cycle), then annealing/elongation for another 26-36 cycles depending on the quality of primers
448 (denature at 94°C for 20 s, annealing/elongation at 55°C for 60 s). Upon the completion of the
449 KASP PCR, reaction plates were read by CFX96 Touch^{TM} Real-time PCR detection system
450 and the data was then analysed with the Allelic Discrimination module of BioRad CFX
451 Manager 3.0. Detected signals were plotted against FAM and HEX fluorescence intensity as a
452 graph, with samples of the same genotype clustering together. To detect SSR markers, PCR
453 products were detected by AATI Fragment Analyzer following the manufacturer's instructions.
454 The primers used for mapping *qKW9* were listed in Supplemental Table S1.

455 Maize plants were examined under natural field conditions in the experimental fields of
456 Wuhan (30°N, 114°E), Sanya (18°N, 109°E), and Baoding (39°N, 115°E) in China. The
457 planting density was 25 cm between adjacent plants in a row and the rows were 60 cm apart.
458 Field management, including irrigation, fertilizer application, and pest control, essentially
459 followed the normal agricultural practices. Harvested maize ears were air-dried and then
460 fully-developed ears were shelled for measuring HKW, KL, and KW as previously reported
461 (Raihan et al., 2016). The t-test with two-tailed and two-sample was used to analyze the
462 phenotype data.

463 **Bacterial artificial chromosome (BAC) screen, sequence, and *de novo* assembly**

464 BACs covering *qKW9* of both parent lines-SK and ZHENG58- were screened. BAC DNA
465 was prepared using the QIAGEN Large-Construct Kit (Cat no: 12462) following the
466 manufacturer's instructions but with 150ml overnight-cultured bacterial input. The recovered
467 DNA was sent to a company (Nextomics Bioscience Co., Ltd, Wuhan, China) for quality
468 control and library construction. The resulting sequence data was assembled by PacBio's
469 open-source SMRT Analysis software.

470 **Fresh weight during the filling stage**

471 NILs derived from homozygous progenies of HIF-p11 were used to analyze the grain
472 filling rate of developing kernels after pollination. NILs with the *qKW9* allele of SK designated
473 as NIL-SK while NILs with the *qKW9* allele of ZHENG58 designated as NIL-ZHENG58.
474 Starting from 6 days after pollination (DAP), 50 fresh kernels were harvested and weighted

475 from 6 ears of each NIL every other day until 30 DAP. At 35 DAP and upon harvest fresh
476 kernels were also weighed. The t-test with two-tailed and two-sample was used to analyze the
477 fresh weight data.

478 **Mutagenesis of *qKW9* with CRISPR/Cas9-based gene editing**

479 Two guide RNA sequences (cggtggtggacatgtactg and ctgttctggggatccagct) against *qKW9*
480 were designed by CRISPR-P 2.0 (http://crispr.hzau.edu.cn/CRISPR2/) then cloned into a
481 CRISPR/Cas9 plant expression vector (Liu et al., 2017a). The backbone of the vector was
482 provided by WIMI Biotechnology Co., Ltd (Changzhou, China). The vector allows expression
483 of single guide RNA by the ZmU61 promoter and Cas9 by a maize UBI promoter. The
484 resulting binary plasmids were transformed into the *Agrobacterium tumefaciens* strain
485 EHA105 and used to transform maize inbred C01. All constructs were sequence-verified. The
486 primers for the genotyping of CRISPR mutants were listed in Supplemental Table S1. Ear
487 weight and kernel weight of CRISPR null alleles and wild type were measure and analyzed by
488 t-test with two-tailed and two-sample.

489

490 **Light Microscopy**

491 Whole sections of mature kernels were stained with iodine solution using the method in a
492 previous report (Zhao et al., 2016). Three different regions of endosperm were examined for
493 the morphology of starch.

494 **Subcellular localization of *qKW9***

495 *Zm00001d048451* was predicted to locate in chloroplast by TargetP (Emanuelsson et al.,
496 2007). To verify this, a codon-optimized CDS (optimized by a web tool -
497 https://www.genscript.com/codon_opt_pr.html) was fused with green fluorescent protein (GFP)
498 and driven by expression from the cauliflowner mosaic virus 35S promoter. The binary
499 vector-pK7FWG2.0-was obtained from Dr. Hannes Claeys (Cold Spring Harbor Laboratory,
500 USA). The plasmids containing the chimeric genes were transferred into Agrobacterium
501 tumefaciens strain GV3101. The resulting strain was co-infiltrated into tobacco (*N. tabacum*)
502 leaves with a strain harboring P19 which was obtained from Dr. Edgar Demesa Arevalo (Cold

503 Spring Harbor Laboratory, USA) (Lindbo, 2007). Fluorescence signals were detected using
504 LSM780. DAPI (4,6-diamidino-2-phenylindole) staining solution
505 (http://cshprotocols.cshlp.org/content/2007/1/pdb.rec10850.full?text_only=true) was injected
506 to the leaf before observing the fluorescence signals. Agrobacterium growth and injection
507 followed the steps described in a previous report (Xu et al., 2015). The primers for building the
508 vector were listed in Supplemental Table S1.

509 **Phylogenetic analysis**

510 To identify the PPR genes in maize B73 RefGen v4, protein sequences of B73 RefGen
511 v4 genes were downloaded from ftp://ftp.gramene.org/pub/gramene/ (B73 RefGen v4.59).
512 Then HMMER 3.0 software (Finn et al., 2011) was used to scan all of the annotated
513 Pentatricopeptide Repeat genes in B73 RefGen v4 with the Midden Markov (HMM) profile
514 of PPR domain (PF01535.20, http://pfam.sanger.ac.uk/) (E-value < 1). Based on the
515 C-terminal domain structure, the HMM profiles of E, E+, and DYW domain were rebuilt
516 using the previously predicted PPR genes in B73 RefGen v3. Then these HMM profiles were
517 used to scan the PPR genes annotated in B73 RefGen v4
518 (ftp://ftp.gramene.org/pub/gramene/CURRENT_RELEASE/gff3/zea_mays/gene_function).
519 Then TargetP version 1.1 (http://www.cbs.dtu.dk/services/TargetP/) was used to predict the
520 organelle targeting of these E, E+, and DYW types PPR proteins. Only the chloroplast
521 targeting genes were kept to conduct the evolutionary analysis with their orthologous genes
522 in Arabidopsis and rice
523 (https://download.maizegdb.org/Zm-B73-REFERENCE-GRAMENE-4.0/Orthologs/). The
524 evolutionary history was inferred using the Neighbor-Joining method (Saitou and Nei, 1987)
525 by MEGAX (Kumar et al., 2018). The bootstrap consensus tree inferred from 500 replicates
526 was taken to represent the evolutionary history of the taxa analyzed (Felsenstein, 1985).

527 **Photosynthetic parameters and chlorophyll content measurements**

528 Carbon dioxide assimilation rate, stomatal conductance, and transpiration rate were
529 measured on fully-expanded maize leaves grown in the field using a portable gas exchange

530 system (LI-6400XT, LI-COR Inc., USA) as described (Huang et al., 2009; Bihmidine et al.,
531 2013). The measurements were conducted at an ambient CO_2 concentration of 400 μmol
532 mol^{-1} and light saturation of 2000 μmol m^{-2} s^{-1}. Leaf photochemical efficiency (Fv/Fm) was
533 measured on dark-adapted leaves using the FlourPen FP100 chlorophyll fluorescence meter
534 (Photon System Instruments, Czech Republic). Leaf chlorophyll content was measured using
535 a chlorophyll meter (SPAD-502, Konica Minolta, Japan). The measurements were performed
536 before pollination and at 22, 30, and 35 days after pollination (DAP) on eight NIL-SK plants
537 or NIL-ZHENG58 plants. Means and standard errors (SE) were calculated using Microsoft
538 Excel. Differences in chlorophyll content and photosynthetic parameters were assessed using
539 the Student's *t*-test embedded in the Microsoft Excel program, at the *P*-value ≤ 0.05 level.

540 **RNA sequencing**

541 To explore the possible RNA editing in leaf by the PPR gene, the ear leaves from NIL-SK
542 and NIL-ZHENG58 plants before pollination and after pollination (22 days and 30 days) were
543 collected. Total RNA was isolated from these samples using Direct-zol RNA MiniPrep Plus kit
544 (Cat no: R2072, ZYMO Research, USA). Libraries were constructed using the Illumina
545 TruSeq Stranded RNA Kit (Illumina, San Diego, CA, USA) following the manufacturer's
546 recommendations. Strand-specific sequencing was performed on the Illumina HiSeq 2000
547 system (paired-end 100-bp reads). The raw reads were trimmed by Trimmomatic v0.36 (Bolger
548 et al., 2014) to gain high-quality clean reads, and the quality of the clean reads was checked
549 using the FASTQC program (Andrews, 2010). Next the clean reads were aligned to maize B73
550 RefGen v4 chloroplast genome by Hisat2 (Kim et al., 2015). Picard tools were subsequently
551 used to add read groups, sort, mark duplicates, and create index
552 (http://broadinstitute.github.io/picard/). Then the GATK was used to call the sequence variants
553 by HaplotypeCaller (McKenna et al., 2010). The ratio of edited allele reads count/total reads
554 count served as editing frequency for each site and the significance of editing frequency
555 difference between NIL-SK and NIL-ZHENG58 was estimated by pairwise *t*-test with a
556 threshold *P*-value < 0.05. Only the loci with a mean editing frequency difference over 5%

557 between NIL-SK and NIL-ZHENG58 were treated as possibly RNA editing sites being
558 affected by *qKW9*.

559 **RNA extraction and qPCR**

560 Total RNA was extracted from various plant tissues except leaf using RNA extraction kit
561 (Cat no: 0416-50, Huayueyang, China). cDNA was synthesized from the extracted RNA using
562 the TransScript One-Step gDNA Removal and cDNA Synthesis SuperMix (Cat no: AT311,
563 TransGen Biotech, China). qPCR was carried out in a total volume of 20 µl containing 2 µl of
564 10x-diluted reverse-transcribed product, 0.2 mM gene-specific primers, and 10 µl KAPA
565 SYBR® FAST qPCR Master Mix (Cat no: KK4607), using a Bio-Rad CFX96 Touch^{TM}
566 Real-time PCR detection system according to the manufacturer's instructions. Quantitative
567 PCR was performed for the gene expression using QPIG, QPPR, and ACTIN primers
568 (Supplemental Table S1).

569 **Immunoblot Analysis**

570 Chloroplast membrane proteins were isolated from the leaves of around 2-week-old
571 maize plants using kits (Cat no: BB-3175, BestBio, China). Protein samples were quantified
572 with BCA protein assay. The protein samples were separated by 12% SDS-PAGE. After
573 electrophoresis, the proteins were transferred onto a PVDF membrane (0.2 µm, Bio-Rad)
574 using Bio-Rad Semi-Dry Transfer Cell. The blot was blocked with 5% v/v milk in TBST for
575 1h at room temperature (RT) with agitation and then incubated in the primary antibody (from
576 Agrisera, AS16 4065) at a dilution of 1: 500 overnight in +4°C. The antibody solution was
577 decanted, and the blot was washed briefly with TBST at RT with agitation. The blot was
578 incubated in secondary antibody (anti-rabbit IgG horseradish peroxidase conjugated, from
579 Agrisera, AS09 602) diluted to 1:10 000 in 1% milk/TBST for 30min at RT with agitation.
580 The blot was washed briefly in TBST at RT with agitation and developed for 2 min with ECL
581 according to the manufacturer's instructions (Cat no: SL1350, Coolaber, China). The signals
582 were visualized by a GeneGnome chemiluminescence analyzer (Syngene).

583 **ACCESSION NUMBERS**

584 Sequence data from this article can be found in the GenBank/NCBI databases under the
585 SRA accession number: PRJNA588870.
586

587 **ACKNOWLEDGEMENTS**

588 This work was supported by the National Key Research and Development Program of China
589 (2016YFD0100303), the National Natural Science Foundation of China (31525017,
590 31961133002), and NSF grant IOS-1546837 to DJ; Juan Huang was sponsored by China
591 Scholarship Council to visit Cold Spring Harbor Laboratory and study in Prof. David Jackson's
592 lab from March 2018 to March 2019 (File No. 201706760027). We thank Dr. Yali Zhang from
593 Shihezi University for suggestions on measurements of chlorophyll fluorescence. We thank Dr.
594 Edgar Demesa Arevalo's help in taking confocal images and for providing for P19 containing
595 strain. We thank Dr. Hannes Claeys for providing pK7FWG2.0 containing strain. We thank
596 Felix Fritschi for use of the chlorophyll fluorescence meter.
597

598 **SUPPLEMENTAL DATA**

599 **Supplemental Figure S1.** Schematic representation of genotypes and kernel weights of
600 recombinant families derived from F1H5.

601 **Supplemental Figure S2.** qPCR analysis of *Zm00001d048450* and *Zm00001d048451*
602 expression.

603 **Supplemental Figure S3.** *qKW9* controls kernel weight majorly by the maternal effect.

604 **Supplemental Table S1.** Primer sequences used in this study.
605
606

607 **Tables**

608 **Table 1.** Ear related and agronomic traits in NIL-SK and NIL-Zheng58.

Trait	NIL-SK		NIL-Zheng58		P-value
	Mean ± SD[a]	N[b]	Mean ± SD	N	
Hundred Kernel Weight/g	15.59 ± 2.01	27	18.57±1.21	30	6.07×10^{-9}
Ear Length/cm	9.75 ± 0.75	31	10.68±0.76	37	3.72×10^{-6}
Kernel Number per Row	22.00±2.99	27	24.03±2.28	32	4.47×10^{-3}
Ear Row Number	12.43±1.00	28	12.39±0.80	36	0.86
Kernel Number per Ear	249.22±39.45	27	279.39±34.28	31	2.89×10^{-3}
Ear Weight/g	43.79±7.60	30	57.33±8.35	36	3.74×10^{-9}
Kernel Weight per Ear/g	38.84±6.60	19	53.68±7.44	17	3.07×10^{-7}
Plant Height/cm	190.73±10.52	92	195.29±10.12	91	3.22×10^{-3}
Ear Height/cm	84.48±7.19	92	83.65±9.68	91	0.51
Days to Shedding/Day	63.38±1.81	68	60.16±1.21	70	6.72×10^{-24}

609 [a] SD=standard deviation; [b]N, number of observed individuals.

610

611 **Table 2** C-to-U editing sites in plastid genes with significant editing frequency difference

612 between NIL-SK and NIL-Zheng58.

Locus(transcript)	Genome position	Feature	Developing Stages	Editing level%		P-value	Editing difference %
				NIL-SK	NIL-Zheng58		
GRMZM5G876106(*ndhB*)	90736	CDS, P>L	Before Pollination	0.00	100.00	NA	100.00
			22 DAP[a]	0.00	100.00		
			30 DAP	0.00	100.00		
GRMZM5G810298 (*ndhB*)	132001	CDS, P>L	Before Pollination	0.00	97.05	2.00E-05	98.15
			22 DAP	0.00	98.79		
			30 DAP	0.00	98.60		
intergenic	65407		Before Pollination	0.00	72.73	0.0041	87.21
			22 DAP	0.00	88.89		
			30 DAP	0.00	100.00		
GRMZM5G866064	139970	CDS, synonymous	Before Pollination	26.64	36.36	0.024	8.96
			22 DAP	18.52	30.60		
			30 DAP	27.87	32.95		
GRMZM5G856777	8558	5'UTR	Before Pollination	9.40	16.77	0.044	5.82
			22 DAP	31.63	39.61		
			30 DAP	35.50	37.63		
GRMZM5G845244 (rps8)	78717	CDS, S>L	Before Pollination	89.36	96.92	0.048	5.79
			22 DAP	98.08	100.00		
			30 DAP	92.11	100.00		

613 [a] DAP= days after pollination.

614

615 **FIGURE LEGENDS**

616 **Figure 1. Plant and kernel morphology of two near-isogenic lines (NILs) of maize,**
617 **NIL-SK (small kernel) and NIL-Zheng58. (A)** NIL-SK (NS) and NIL-Zheng58 (NZ) had
618 very similar plant architecture, Bar=20cm. **(B)** NS 2-week old seedlings were smaller than NZ.
619 Bar=4 cm. **(C)** Leaf senescence was greater in NS at 30 days after pollination compared with
620 NZ. Bar=10 cm. **(D)** Ears of NS were smaller than in NZ. Bar=1 cm. **(E) to (J)** Mature kernels
621 of NS (E-G) were smaller that in NZ (H-J). Whole kernels of NS and NZ (**[E]** and **[H]**).
622 Bar=2mm; transverse section of kernel of NS and NZ (**[F]** and **[I]**). Bar=2 mm; Longitudinal
623 section of kernel of NS and NZ (**[G]** and **[J]**). Bar=2 mm; **(K) to (R)** Similar starch structure in
624 endosperms of mature kernels of NS and NZ. Whole longitudinal section stained with iodine
625 solution of kernels of NS and NZ (**[K]** and **[O]**), 1, 2, 3 indicate the crown, farinaceous and
626 keratin endosperm regions, respectively. Bar=1 mm; **(L)** to **(N)** correspond to regions 1, 2, 3 in
627 **(K)**; and **(P)** to **(R)** correspond to regions 1, 2, 3 in **(O)**. Bar=10 μm.

628

629 **Figure 2. Fine mapping and gene structure of *qKW9*. (A)** Mapping delimits *qKW9* to the
630 region between M3484 and M3506 on chromosome 9. F1H5, which derives from ZHENG58 ×
631 SK (small kernel) recombinant inbred line (RIL) population, the founder line for screening
632 heterozygous inbred families (HIFs) for fine mapping *qKW9*. Progeny tests of kernel weight
633 were conducted on the resulting recombinant families. White bar represents the homozygous
634 chromosomal segment for SK, gray bar represents the heterozygous chromosomal segment for
635 ZHENG58 × SK, black bar represents the homozygous chromosomal segment for ZHENG58.
636 The graphical genotype represents F1H5. Numbers between markers represent physical
637 distances (Kb) between the adjacent markers and numbers in brackets represent the number
638 of recombinants. **(B)** Gene annotations in the region of *qKW9* of B73, SK, and Zheng58.
639 Sequences were obtained by sequencing bacterial artificial chromosomes (BACs) covering
640 *qKW9* from SK and ZHENG58 genome BAC libraries, respectively. Zm00001d048452 was
641 absent in both SK and ZHENG58. Two candidate genes-*Zm00001d048450* and
642 *Zm00001d048451*-were identified in *qKW9*. **(C)** *Zm00001d048451* is an 1.8kb intron-less gene

643 with eight pentatricopeptide repeats; a 13-bp deletion was identified in the coding region of
644 *Zm00001d048451* in SK. CRISPR/Cas9 gene editing technology was used to create knockout
645 mutants with a single guide sequence (the 20-bp sequence adjacent to PAM) targeting
646 *Zm00001d048451* in the inbred C01. Two mutated alleles, *qkw9-cr1* and *qkw9-cr2*, were
647 identified by sequencing the first-generation (T_0) plants and used for further genetic analysis.
648
649 **Figure 3. Two CRISPR/Cas9 knockout mutants of *Zm00001d048451-qkw9-cr1* and**
650 ***qkw9-cr2*-produced smaller ears and smaller kernels than wild type.** Each mutant is shown
651 alongside its corresponding wild type (WT) segregant from a single Cas9-free T_1 generation
652 plant. **(A)** and **(B):** comparison of ears produced by CRISPR/Cas9 mutants (left) and WT
653 (right). *qkw9-cr1* (left) and WT (right) in **(A)** and *qkw9-cr2* (left) and WT (right) in **(B)**.
654 Bar=1 cm. **(D)** and **(E)** kernels produced by CRISPR/Cas9 mutants (lower row) were smaller
655 than WT (upper row). *qkw9-cr1* (lower) and wild type (upper) in **(D)** and *qkw9-cr2* (lower) and
656 WT (upper) in **(E)**. Bar=1 cm. **(C)** and **(F)** show reductions in ear weight **(C)** and kernel weight
657 **(F)** of CRISPR/Cas9 knockout mutants. Data are shown as mean ± SD; N = 6 for each
658 genotype; *** $P < 0.001$, two-tailed, two-sample t-test.
659
660 **Figure 4. Characterization of *qKW9*/*Zm00001d048451*. (A)** Phylogenetic tree of maize,
661 Arabidopsis and rice PLS-E, PLE-E+, and PLS-DYW Pentatricopeptide Repeat genes
662 predicted to localize in chloroplast/plastid by TargetP. Scale bar represent branch length. **(B)**
663 Autofluorescence of chlorophyll (red). **(C)** qKW9-GFP fusion protein (green) in green puncta
664 within plastids. **(D)** DAPI (4′,6-diamidino-2-phenylindole) staining (blue) of nuclei. **(E)**
665 Overlay of **(B)**, **(C)** and **(D)**. Scale bar=5 µm. **(F)** Allele in the near-isogenic line NIL-SK
666 (small kernel) of *Zm00001d048451* fails to edit C to U in 246th codon of *ndhB* gene. C-to-U
667 editing in *ndhB-246* results in amino acid change from proline to leucine. NIL-Zheng58,
668 near-isogenic line Zheng58; Pro, proline; Leu, leucine.
669
670 **Figure 5. Protein blot analysis of the** NADH dehydrogenase-like **(NDH) complex.**

671 Chloroplast membrane protein was extracted with a commercial kit and protein samples were
672 quantified with bicinchoninic acid (BCA) protein assay. 1× sample amount equals 40 μg
673 protein. Antibody against NdhH was used to indicate the amount of NDH complex.
674 Chloroplast membrane protein from the near-isogenic line Zheng58 (NIL-ZHENG58) was
675 loaded a series of dilutions as indicated. Specific bands corresponded in size of NdhH protein
676 (expected in 45 kDa, apparent in 49 kDa). Signals in NIL-ZHENG58 declined along with the
677 dilution. The level of NdhH in NIL-SK (small kernel) was reduced to less than 25% of
678 NIL-ZHENG58. Coomassie R-250 staining was used to show the proteins separated by
679 electropheris as a loading control.
680
681 **Figure 6**. NADH dehydrogenase-like **(NDH) activity monitoring, and non-photochemical**
682 **quenching (NPQ) and electron transport rate (ETR) in null mutants of *qKW9*. (A)**
683 Monitoring of NDH activity using chlorophyll fluorescence analysis for *qkw9-cr1* and
684 *qkw9-cr2* mutants. The curve shows the typical change trace of chlorophyll fluorescence *in*
685 *vivo* as the NDH complex catalyzes the post-illumination reduction of the plastoquinone pool
686 (Okuda et al., 2007). The change in post-illumination fluorescence ascribed to NDH activity
687 was different between wild type (WT) and mutants. Insets are magnified traces from the
688 boxed area. ML, measuring light; AL, actinic light; SP, a saturating pulse of white light. Eight
689 plants were measured for each WT and mutants. **(B)** NPQ was induced by light intensity in
690 both *cr*1 and WT, but it was significantly lower in *cr*1 under photon flux density of
691 2413 μmol of photons $m^{-2}s^{-1}$. Data are shown as mean ± SD; N=6 for each genotype; *** $P <$
692 0.001, two-tailed and two-sample t-test. **(C)** Relative ETR (rETR) under different photon flux
693 densities. rETR in cr1 and WT reached maximum when the light intensity was 422 μmol of
694 photons $m^{-2}s^{-1}$. It was significantly lower in *cr*1 under the photon flux density of 206 μmol of
695 photons $m^{-2}s^{-1}$ and 2413 μmol of photons $m^{-2}s^{-1}$. The rETR is depicted relative to a maximal
696 value of ϕ_{PSII} × PPFD (photon flux density, μmol of photons $m^{-2}s^{-1}$). Data are shown as mean ±
697 SD; N=6 for each genotype; * $P < 0.05$, two-tailed and two-sample t-test.
698

699 **Figure 7**. **Grain filling and photosynthesis measurement in two near-isogenic lines (NILs),**
700 **NIL-SK (small kernel) and NIL-Zheng58. (A)** Time courses of fresh weight of 50 kernels of
701 NIL-SK and NIL-Zheng58. The fresh weight of NIL-SK and NIL-ZHEGN58 reached the
702 maximum at 30 days after pollination (DAP) and 35 DAP, respectively. **(B)** to **(E)** Time
703 courses of photosynthesis-rate related parameters of NIL-SK and NIL-Zheng58. Net
704 photosynthesis **(B)**, stomatal conductance (C), and transpiration rate **(D)** were significantly
705 lower in NIL-SK than NIL-ZHENG58 at 22 DAP and 30 DAP; **(E)** chlorophyll content and **(F)**
706 maximum photochemical efficiency did not show significant between genotype differences at
707 any of the four stages tested. Data are shown as mean ± SD; N=6 for each genotype; * $P < 0.05$,
708 ** $P < 0.01$, *** $P < 0.001$, two-tailed and two-sample t-test.

709

Parsed Citations

Alric J, Johnson X (2017) Alternative electron transport pathways in photosynthesis: a confluence of regulation. Curr Opin Plant Biol 37: 78–86
Pubmed: Author and Title
Google Scholar: Author Only Title Only Author and Title

Andrews S (2010) FastQC: a quality control tool for high throughput sequence data.

Barkan A, Small I (2014) Pentatricopeptide Repeat Proteins in Plants. Annu Rev Plant Biol 65: 415–442
Pubmed: Author and Title
Google Scholar: Author Only Title Only Author and Title

Bihmidine S, Hunter CT, Johns CE, Koch KE, Braun DM (2013) Regulation of assimilate import into sink organs: Update on molecular drivers of sink strength. Front Plant Sci. doi: 10.3389/fpls.2013.00177
Pubmed: Author and Title
Google Scholar: Author Only Title Only Author and Title

Bolger AM, Lohse M, Usadel B (2014) Trimmomatic: A flexible trimmer for Illumina sequence data. Bioinformatics 30: 2114–2120
Pubmed: Author and Title
Google Scholar: Author Only Title Only Author and Title

Burrows PA, Sazanov LA, Svab Z, Maliga P, Nixon PJ (1998) Identification of a functional respiratory complex in chloroplasts through analysis of tobacco mutants containing disrupted plastid ndh genes. EMBO J 17: 868–876
Pubmed: Author and Title
Google Scholar: Author Only Title Only Author and Title

Cai M, Li S, Sun F, Sun Q, Zhao H, Ren X, Zhao Y, Tan BC, Zhang Z, Qiu F (2017) Emp10 encodes a mitochondrial PPR protein that affects the cis-splicing of nad2 intron 1 and seed development in maize. Plant J 91: 132–144
Pubmed: Author and Title
Google Scholar: Author Only Title Only Author and Title

Chateigner-Boutin AL, Small I (2010) Plant RNA editing. RNA Biol 7: 213–219
Pubmed: Author and Title
Google Scholar: Author Only Title Only Author and Title

Chen X, Feng F, Qi W, Xu L, Yao D, Wang Q, Song R (2017) Dek35 Encodes a PPR Protein that Affects cis-Splicing of Mitochondrial nad4 Intron 1 and Seed Development in Maize. Mol Plant 10: 427–441
Pubmed: Author and Title
Google Scholar: Author Only Title Only Author and Title

Clark JK, Sheridan F (1991) Isolation and Characterization of 51 embryo-specific Mutations of Maize. Plant Cell 3: 935–951
Pubmed: Author and Title
Google Scholar: Author Only Title Only Author and Title

Dai D, Luan S, Chen X, Wang Q, Feng Y, Zhu C, Qi W, Song R (2018) Maize Dek37 encodes a P-type PPR protein that affects cis-splicing of mitochondrial nad2 intron 1 and seed development. Genetics 208: 1069–1082
Pubmed: Author and Title
Google Scholar: Author Only Title Only Author and Title

DalCorso G, Pesaresi P, Masiero S, Aseeva E, Schünemann D, Finazzi G, Joliot P, Barbato R, Leister D (2008) A Complex Containing PGRL1 and PGR5 Is Involved in the Switch between Linear and Cyclic Electron Flow in Arabidopsis. Cell 132: 273–285
Pubmed: Author and Title
Google Scholar: Author Only Title Only Author and Title

Emanuelsson O, Brunak S, von Heijne G, Nielsen H (2007) Locating proteins in the cell using TargetP, SignalP and related tools. Nat Protoc 2: 953–971
Pubmed: Author and Title
Google Scholar: Author Only Title Only Author and Title

Felsenstein J (1985) Confidence Limits on Phylogenies: An Approach Using the Bootstrap. Evolution (N Y) 39: 783
Pubmed: Author and Title
Google Scholar: Author Only Title Only Author and Title

Finn RD, Clements J, Eddy SR (2011) HMMER web server: Interactive sequence similarity searching. Nucleic Acids Res. doi: 10.1093/nar/gkr367
Pubmed: Author and Title
Google Scholar: Author Only Title Only Author and Title

Hammani K, Okuda K, Tanz SK, Chateigner-Boutin A-L, Shikanai T, Small I (2009) A Study of New Arabidopsis Chloroplast RNA Editing Mutants Reveals General Features of Editing Factors and Their Target Sites. Plant Cell 21: 3686–3699
Pubmed: Author and Title
Google Scholar: Author Only Title Only Author and Title

Hashimoto M, Endo T, Peltier G, Tasaka M, Shikanai T, Wise RP, Pring DR (2003) A nucleus-encoded factor, CRR2, is essential for the expression of chloroplast ndhB in Arabidopsis. Plant J 36: 541–549
Pubmed: Author and Title
Google Scholar: Author Only Title Only Author and Title

Horváth EM, Peter SO, Joët T, Rumeau D, Cournac L, Horváth G V., Kavanagh TA, Schäfer C, Peltier G, Medgyesy P (2000) Targeted Inactivation of the Plastid ndhB Gene in Tobacco Results in an Enhanced Sensitivity of Photosynthesis to Moderate Stomatal Closure. Plant Physiol 123: 1337–1350
Pubmed: Author and Title
Google Scholar: Author Only Title Only Author and Title

Huang M, Slewinski TL, Baker RF, Janick-Buckner D, Buckner B, Johal GS, Braun DM (2009) Camouflage patterning in maize leaves results from a defect in porphobilinogen deaminase. Mol Plant 2: 773–789
Pubmed: Author and Title
Google Scholar: Author Only Title Only Author and Title

Ishikawa N, Takabayashi A, Noguchi K, Tazoe Y, Yamamoto H, Von Caemmerer S, Sato F, Endo T (2016a) NDH-mediated cyclic electron flow around photosystem I is crucial for C4 photosynthesis. Plant Cell Physiol 57: 2020–2028
Pubmed: Author and Title
Google Scholar: Author Only Title Only Author and Title

Ishikawa N, Takabayashi A, Sato F, Endo T (2016b) Accumulation of the components of cyclic electron flow around photosystem I in C4 plants, with respect to the requirements for ATP. Photosynth Res 129: 261–277
Pubmed: Author and Title
Google Scholar: Author Only Title Only Author and Title

Karcher D, Bock R (2002) The amino acid sequence of a plastid protein is developmentally regulated by RNA editing. J Biol Chem 277: 5570–5574
Pubmed: Author and Title
Google Scholar: Author Only Title Only Author and Title

Kim D, Langmead B, Salzberg SL (2015) HISAT: A fast spliced aligner with low memory requirements. Nat Methods 12: 357–360
Pubmed: Author and Title
Google Scholar: Author Only Title Only Author and Title

Kotera E, Tasaka M, Shikanai T (2005) A pentatricopeptide repeat protein is essential for RNA editing in chloroplasts. Nature 433: 326–330
Pubmed: Author and Title
Google Scholar: Author Only Title Only Author and Title

Kumar S, Stecher G, Li M, Knyaz C, Tamura K (2018) MEGA X: Molecular evolutionary genetics analysis across computing platforms. Mol Biol Evol 35: 1547–1549
Pubmed: Author and Title
Google Scholar: Author Only Title Only Author and Title

Laughlin TG, Bayne AN, Trempe J-F, Savage DF, Davies KM (2019) Structure of the complex I-like molecule NDH of oxygenic photosynthesis. Nature 566: 411–414
Pubmed: Author and Title
Google Scholar: Author Only Title Only Author and Title

Li Q, Li L, Yang X, Warburton ML, Bai G, Dai J, Li J, Yan J (2010a) Relationship, evolutionary fate and function of two maize co-orthologs of rice GW2 associated with kernel size and weight. BMC Plant Biol 10: 143
Pubmed: Author and Title
Google Scholar: Author Only Title Only Author and Title

Li Q, Yang X, Bai G, Warburton ML, Mahuku G, Gore M, Dai J, Li J, Yan J (2010b) Cloning and characterization of a putative GS3 ortholog involved in maize kernel development. Theor Appl Genet 120: 753–763
Pubmed: Author and Title
Google Scholar: Author Only Title Only Author and Title

Li X, Gu W, Sun S, Chen Z, Chen J, Song W, Zhao H, Lai J (2018) Defective Kernel 39 encodes a PPR protein required for seed development in maize. J Integr Plant Biol 60: 45–64
Pubmed: Author and Title
Google Scholar: Author Only Title Only Author and Title

Li XJ, Zhang YF, Hou M, Sun F, Shen Y, Xiu ZH, Wang X, Chen ZL, Sun SSM, Small I, et al (2014) Small kernel 1 encodes a pentatricopeptide repeat protein required for mitochondrial nad7 transcript editing and seed development in maize (Zea mays) and rice (Oryza sativa). Plant J 79: 797–809
Pubmed: Author and Title
Google Scholar: Author Only Title Only Author and Title

Lindbo JA (2007) High-efficiency protein expression in plants from agroinfection-compatible Tobacco mosaic virus expression vectors. BMC Biotechnol 7: 1–11
Pubmed: Author and Title
Google Scholar: Author Only Title Only Author and Title

Liu H, Ding Y, Zhou Y, Jin W, Xie K, Chen LL (2017a) CRISPR-P 2.0: An Improved CRISPR-Cas9 Tool for Genome Editing in Plants. Mol Plant 10: 530–532
Pubmed: Author and Title
Google Scholar: Author Only Title Only Author and Title

Liu J, Deng M, Guo H, Raihan S, Luo J, Xu Y, Dong X, Yan J (2015) Maize orthologs of rice GS5 and their trans-regulator are associated with kernel development. J Integr Plant Biol 57: 943–953
Pubmed: Author and Title
Google Scholar: Author Only Title Only Author and Title

Liu J, Huang J, Guo H, Lan L, Wang H, Xu Y, Yang X, Li W, Tong H, Xiao Y, et al (2017b) The conserved and unique genetic architecture of kernel size and weight in maize and rice. Plant Physiol 175: 774–785
Pubmed: Author and Title
Google Scholar: Author Only Title Only Author and Title

Liu N, Liu J, Li W, Pan Q, Liu J, Yang X, Yan J, Xiao Y (2018) Intraspecific variation of residual heterozygosity and its utility for quantitative genetic studies in maize. BMC Plant Biol 18: 66
Pubmed: Author and Title
Google Scholar: Author Only Title Only Author and Title

Lurin C, Andres C, Aubourg S, Bellaoui M, Bitton F, Bruyere C, Caboche M, Debast C, Gualberto J, Hoffmann H, et al (2004) Genome-wide Analysis of Arabidopsis Pentatricopeptide Repeat Proteins Reveals Their Essential Role in Organelle Biogenesis. Plant Cell 16: 2089–2103
Pubmed: Author and Title
Google Scholar: Author Only Title Only Author and Title

Maier RM, Neckermann K, Igloi GL, Koössel H (1995) Complete sequence of the maize chloroplast genome: Gene content, hotspots of divergence and fine tuning of genetic information by transcript editing. J Mol Biol 251: 614–628
Pubmed: Author and Title
Google Scholar: Author Only Title Only Author and Title

Manavski N, Guyon V, Meurer J, Wienand U, Brettschneider R (2012) An Essential Pentatricopeptide Repeat Protein Facilitates 5' Maturation and Translation Initiation of rps3 mRNA in Maize Mitochondria. Plant Cell 24: 3087–3105
Pubmed: Author and Title
Google Scholar: Author Only Title Only Author and Title

McCarty DR (2017) Maize kernel development. In B Larkins, ed, Maize kernel Dev. CABI, pp 44–55
Pubmed: Author and Title
Google Scholar: Author Only Title Only Author and Title

McKenna A, Hanna M, Banks E, Sivachenko A, Cibulskis K, Kernytsky A, Garimella K, Altshuler D, Gabriel S, Daly M, et al (2010) The genome analysis toolkit: A MapReduce framework for analyzing next-generation DNA sequencing data. Genome Res 20: 1297–1303
Pubmed: Author and Title
Google Scholar: Author Only Title Only Author and Title

Munekage Y, Hashimoto M, Miyake C, Tomizawa KI, Endo T, Tasaka M, Shikanai T (2004) Cyclic electron flow around photosystem I is essential for photosynthesis. Nature 429: 579–582
Pubmed: Author and Title
Google Scholar: Author Only Title Only Author and Title

Munekage Y, Hojo M, Meurer J, Endo T, Tasaka M, Shikanai T (2002) PGR5 is involved in cyclic electron flow around photosystem I and is essential for photoprotection in Arabidopsis. Cell 110: 361–371
Pubmed: Author and Title
Google Scholar: Author Only Title Only Author and Title

Munekage YN, Taniguchi YY (2016) Promotion of Cyclic Electron Transport Around Photosystem I with the Development of C4 Photosynthesis. Plant Cell Physiol 57: 897–903
Pubmed: Author and Title
Google Scholar: Author Only Title Only Author and Title

Nakamura N, Iwano M, Havaux M, Yokota A, Munekage YN (2013) Promotion of cyclic electron transport around photosystem I during the evolution of NADP-malic enzyme-type C4 photosynthesis in the genus Flaveria. New Phytol 199: 832–842
Pubmed: Author and Title
Google Scholar: Author Only Title Only Author and Title

Nakano H, Yamamoto H, Shikanai T (2019) contribution of NDH-dependent cyclic electron transport around photosyst. BBA-Bioenergetics 1860: 369–374
Pubmed: Author and Title
Google Scholar: Author Only Title Only Author and Title

Nashilevitz S, Melamed-Bessudo C, Izkovich Y, Rogachev I, Osorio S, Itkin M, Adato A, Pankratov I, Hirschberg J, Fernie AR, et al (2010) An orange ripening mutant links plastid NAD(P)H dehydrogenase complex activity to central and specialized metabolism during tomato fruit maturation. Plant Cell 22: 1977–1997

Pubmed: Author and Title
Google Scholar: Author Only Title Only Author and Title

Neuffer MG, Sheridan WF (1980) DEFECTIVE KERNEL MUTANTS OF MAIZE . I . GENETIC AND LETHALITY STUDIES. Genetics 95: 929–944
Pubmed: Author and Title
Google Scholar: Author Only Title Only Author and Title

Okuda K, Chateigner-Boutin A-L, Nakamura T, Delannoy E, Sugita M, Myouga F, Motohashi R, Shinozaki K, Small I, Shikanai T (2009) Pentatricopeptide Repeat Proteins with the DYW Motif Have Distinct Molecular Functions in RNA Editing and RNA Cleavage in Arabidopsis Chloroplasts . Plant Cell 21: 146–156
Pubmed: Author and Title
Google Scholar: Author Only Title Only Author and Title

Okuda K, Hammani K, Tanz SK, Peng L, Fukao Y, Myouga F, Motohashi R, Shinozaki K, Small I, Shikanai T (2010) The pentatricopeptide repeat protein OTP82 is required for RNA editing of plastid ndhB and ndhG transcripts. Plant J 61: 339–349
Pubmed: Author and Title
Google Scholar: Author Only Title Only Author and Title

Okuda K, Myouga F, Motohashi R, Shinozaki K, Shikanai T (2007) Conserved domain structure of pentatricopeptide repeat proteins involved in chloroplast RNA editing. Proc Natl Acad Sci 104: 8178–8183
Pubmed: Author and Title
Google Scholar: Author Only Title Only Author and Title

Peeters NM, Hanson MR (2002) Transcript abundance supercedes editing efficiency as a factor in developmental variation of chloroplast gene expression. RNA 8: 497–511
Pubmed: Author and Title
Google Scholar: Author Only Title Only Author and Title

Peltier G, Aro E, Shikanai T (2016) NDH-1 and NDH-2 Plastoquinone Reductases in Oxygenic Photosynthesis. Annu Rev Plant Biol 67: 55–80
Pubmed: Author and Title
Google Scholar: Author Only Title Only Author and Title

Peterson RB, Schultes NP, McHale NA, Zelitch I (2016) Evidence for a Role for NAD(P)H Dehydrogenase in Concentration of CO2 in the Bundle Sheath Cell of Zea mays. Plant Physiol 171(1):125-38. doi: 10.1104/pp.16.00120
Pubmed: Author and Title
Google Scholar: Author Only Title Only Author and Title

Qi W, Tian Z, Lu L, Chen X, Chen X, Zhang W, Song R (2017) Editing of mitochondrial transcripts nad3 and cox2 by dek10 is essential for mitochondrial function and maize plant development. Genetics 205: 1489–1501
Pubmed: Author and Title
Google Scholar: Author Only Title Only Author and Title

Raihan MS, Liu J, Huang J, Guo H, Pan Q, Yan J (2016) Multi-environment QTL analysis of grain morphology traits and fine mapping of a kernel-width QTL in Zheng58 × SK maize population. Theor Appl Genet 129: 1465–1477
Pubmed: Author and Title
Google Scholar: Author Only Title Only Author and Title

Ren X, Pan Z, Zhao H, Zhao J, Cai M, Li J, Zhang Z, Qiu F, Leubner G (2017) EMPTY PERICARP11 serves as a factor for splicing of mitochondrial nad1 intron and is required to ensure proper seed development in maize. J Exp Bot 68: 4571–4581
Pubmed: Author and Title
Google Scholar: Author Only Title Only Author and Title

Rumeau D, Peltier G, Cournac L (2007) Chlororespiration and cyclic electron flow around PSI during photosynthesis and plant stress response. Plant, Cell Environ 30: 1041–1051
Pubmed: Author and Title
Google Scholar: Author Only Title Only Author and Title

Ruwe H, Castandet B, Schmitz-Linneweber C, Stern DB (2013) Arabidopsis chloroplast quantitative editotype. FEBS Lett 587: 1429–1433
Pubmed: Author and Title
Google Scholar: Author Only Title Only Author and Title

Ruwe H, Gutmann B, Schmitz-Linneweber C, Small I, Kindgren P (2019) The E domain of CRR2 participates in sequence-specific recognition of RNA in plastids. New Phytol 222: 218–229
Pubmed: Author and Title
Google Scholar: Author Only Title Only Author and Title

Saitou N, Nei M (1987) The neighbor-joining method: a new method for reconstructing phylogenetic trees. Mol Biol Evol 4: 406–425
Pubmed: Author and Title
Google Scholar: Author Only Title Only Author and Title

Scanlon MJ, Takacs EM (2009) Kernel biology. In J Bennetzen, S Hake, eds, Handb. Maize Its Biol. Springer, New York, NY, pp 121–143
Pubmed: Author and Title

Google Scholar: Author Only Title Only Author and Title

Schmitz-Linneweber C, Small I (2008) Pentatricopeptide repeat proteins: a socket set for organelle gene expression. Trends Plant Sci 13: 663–670
Pubmed: Author and Title
Google Scholar: Author Only Title Only Author and Title

Sheridan WF, Neuffer MG (1980) Defective kernel mutants of maize II. morphological and embryo culture studies. Genetics 95: 945–960
Pubmed: Author and Title
Google Scholar: Author Only Title Only Author and Title

Shikanai T (2007) Cyclic Electron Transport Around Photosystem I: Genetic Approaches. Annu Rev Plant Biol 58: 199–217
Pubmed: Author and Title
Google Scholar: Author Only Title Only Author and Title

Shikanai T, Endo T, Hashimoto T, Yamada Y, Asada K, Yokota A (1998) Directed disruption of the tobacco ndhB gene impairs cyclic electron flow around photosystem I. Proc Natl Acad Sci 95: 9705–9709
Pubmed: Author and Title
Google Scholar: Author Only Title Only Author and Title

Sonnewald U, Fernie AR (2018) Next-generation strategies for understanding and influencing source–sink relations in crop plants. Curr Opin Plant Biol 43: 63–70
Pubmed: Author and Title
Google Scholar: Author Only Title Only Author and Title

Sosso D, Luo D, Li Q-B, Sasse J, Yang J, Gendrot G, Suzuki M, Koch KE, McCarty DR, Chourey PS, et al (2015) Seed filling in domesticated maize and rice depends on SWEET-mediated hexose transport. Nat Genet 47: 1489–1493
Pubmed: Author and Title
Google Scholar: Author Only Title Only Author and Title

Sosso D, Mbelo S, Vernoud V, Gendrot G, Dedieu A, Chambrier P, Dauzat M, Heurtevin L, Guyon V, Takenaka M, et al (2012) PPR2263, a DYW-Subgroup Pentatricopeptide Repeat Protein, Is Required for Mitochondrial nad5 and cob Transcript Editing, Mitochondrion Biogenesis, and Maize Growth. Plant Cell 24: 676–691
Pubmed: Author and Title
Google Scholar: Author Only Title Only Author and Title

South PF, Cavanagh AP, Liu HW, Ort DR (2019) Synthetic glycolate metabolism pathways stimulate crop growth and productivity in the field. Science (80-) 363: eaat9077
Pubmed: Author and Title
Google Scholar: Author Only Title Only Author and Title

Stelpflug SC, Sekhon RS, Vaillancourt B, Hirsch CN, Buell CR, de Leon N, Kaeppler SM (2016) An expanded maize gene expression atlas based on RNA sequencing and its use to explore root development. Plant Genome. doi: 10.3835/plantgenome2015.04.0025
Pubmed: Author and Title
Google Scholar: Author Only Title Only Author and Title

Strand DD, Fisher N, Kramer DM (2017) The higher plant plastid NAD(P)H dehydrogenase-like complex (NDH) is a high efficiency proton pump that increases ATP production by cyclic electron flow. J Biol Chem 292: 11850–11860
Pubmed: Author and Title
Google Scholar: Author Only Title Only Author and Title

Sun F, Wang X, Bonnard G, Shen Y, Xiu Z, Li X, Gao D, Zhang Z, Tan BC (2015) Empty pericarp7 encodes a mitochondrial E-subgroup pentatricopeptide repeat protein that is required for ccmFN editing, mitochondrial function and seed development in maize. Plant J 84: 283–295
Pubmed: Author and Title
Google Scholar: Author Only Title Only Author and Title

Sun F, Xiu Z, Jiang R, Liu Y, Zhang X, Yang Y, Li X (2019) The mitochondrial pentatricopeptide repeat protein EMP12 is involved in the splicing of three nad2 introns and seed development in maize. J Exp Bot 70: 963–972
Pubmed: Author and Title
Google Scholar: Author Only Title Only Author and Title

Takabayashi A, Kishine M, Asada K, Endo T, Sato F (2005) Differential use of two cyclic electron flows around photosystem I for driving CO2-concentration mechanism in C4 photosynthesis. Proc Natl Acad Sci 102: 16898–16903
Pubmed: Author and Title
Google Scholar: Author Only Title Only Author and Title

Trapnell C, Roberts A, Goff L, Pertea G, Kim D, Kelley DR, Pimentel H, Salzberg SL, Rinn JL, Pachter L (2012) Differential gene and transcript expression analysis of RNA-seq experiments with TopHat and Cufflinks. Nat Protoc 7: 562–578
Pubmed: Author and Title
Google Scholar: Author Only Title Only Author and Title

Tsudzuki T, Wakasugi T, Sugiura M (2001) Comparative analysis of RNA editing sites in higher plant chloroplasts. J Mol Evol 53: 327–332
Pubmed: Author and Title

Google Scholar: Author Only Title Only Author and Title

Wang H, Nussbaum-Wagler T, Li B, Zhao Q, Vigouroux Y, Faller M, Bomblies K, Lukens L, Doebley JF (2005) The origin of the naked grains of maize. Nature 436: 714–719
Pubmed: Author and Title
Google Scholar: Author Only Title Only Author and Title

Wang H, Studer AJ, Zhao Q, Meeley R, Doebley JF (2015) Evidence that the origin of naked kernels during maize domestication was caused by a single amino acid substitution in tga1. Genetics 200: 965–974
Pubmed: Author and Title
Google Scholar: Author Only Title Only Author and Title

Wang P, Duan W, Takabayashi A, Endo T, Shikanai T, Ye J-Y, Mi H (2006) Chloroplastic NAD(P)H Dehydrogenase in Tobacco Leaves Functions in Alleviation of Oxidative Damage Caused by Temperature Stress. Plant Physiol 141: 465–474
Pubmed: Author and Title
Google Scholar: Author Only Title Only Author and Title

Wu A, Hammer GL, Doherty A, von Caemmerer S, Farquhar GD (2019) Quantifying impacts of enhancing photosynthesis on crop yield. Nat Plants 5: 380–388
Pubmed: Author and Title
Google Scholar: Author Only Title Only Author and Title

Xiu Z, Sun F, Shen Y, Zhang X, Jiang R, Bonnard G, Zhang J, Tan BC (2016) EMPTY PERICARP16 is required for mitochondrial nad2 intron 4 cis-splicing, complex i assembly and seed development in maize. Plant J 85: 507–519
Pubmed: Author and Title
Google Scholar: Author Only Title Only Author and Title

Xu F, Copeland C, Li X (2015) Protein Immunoprecipitation Using Nicotiana benthamiana Transient Expression System. Bio-protocol 5: e1520
Pubmed: Author and Title
Google Scholar: Author Only Title Only Author and Title

Yagi Y, Tachikawa M, Noguchi H, Satoh S, Obokata J, Nakamura T (2013) Pentatricopeptide repeat proteins involved in plant organellar RNA editing. RNA Biol 10: 1419–1425
Pubmed: Author and Title
Google Scholar: Author Only Title Only Author and Title

Yamori W, Makino A, Shikanai T (2016) A physiological role of cyclic electron transport around photosystem I in sustaining photosynthesis under fluctuating light in rice. Sci Rep 6: 1–12
Pubmed: Author and Title
Google Scholar: Author Only Title Only Author and Title

Yamori W, Shikanai T, Makino A (2015) Photosystem i cyclic electron flow via chloroplast NADH dehydrogenase-like complex performs a physiological role for photosynthesis at low light. Sci Rep 5: 13908
Pubmed: Author and Title
Google Scholar: Author Only Title Only Author and Title

Yang N, Liu J, Gao Q, Gui S, Chen L, Yang L, Huang J, Deng T, Luo J, He L, et al (2019) Genome assembly of a tropical maize inbred line provides insights into structural variation and crop improvement. Nat Genet 51: 1052–1059
Pubmed: Author and Title
Google Scholar: Author Only Title Only Author and Title

Yin X, Struik PC (2018) The energy budget in C4 photosynthesis: insights from a cell-type-specific electron transport model. New Phytol 218: 986–998
Pubmed: Author and Title
Google Scholar: Author Only Title Only Author and Title

Zhao L, Pan T, Cai C, Wang J, Wei C (2016) Application of whole sections of mature cereal seeds to visualize the morphology of endosperm cell and starch and the distribution of storage protein. J Cereal Sci 71: 19–27
Pubmed: Author and Title
Google Scholar: Author Only Title Only Author and Title